

A Large-scale AI-generated Image Inpainting Benchmark

Paschalis Giakoumoglou^{1,2} Dimitrios Karageorgiou²
Symeon Papadopoulos² Panagiotis C. Petrantonis¹

¹Department of Electrical and Computer Engineering, Aristotle University of Thessaloniki

²Information Technologies Institute, CERTH

{giakoupg, ppetrant}@ece.auth.gr, {giakoupg, dkarageo, papadop}@iti.gr

Abstract

*Recent advances in generative models enable highly realistic image manipulations, creating an urgent need for robust forgery detection methods. Current datasets for training and evaluating these methods are limited in scale and diversity. To address this, we propose a methodology for creating high-quality inpainting datasets and apply it to create **DiQuID**, comprising over 95,000 inpainted images generated from 78,000 original images sourced from MS-COCO, RAISE, and OpenImages. Our methodology consists of three components: (1) Semantically Aligned Object Replacement (SAOR) that identifies suitable objects through instance segmentation and generates contextually appropriate prompts, (2) Multiple Model Image Inpainting (MMII) that employs various state-of-the-art inpainting pipelines primarily based on diffusion models to create diverse manipulations, and (3) Uncertainty-Guided Deceptiveness Assessment (UGDA) that evaluates image realism through comparative analysis with originals. The resulting dataset surpasses existing ones in diversity, aesthetic quality, and technical quality. We provide comprehensive benchmarking results using state-of-the-art forgery detection methods, demonstrating the dataset’s effectiveness in evaluating and improving detection algorithms. Through a human study with 42 participants on 1,000 images, we show that while humans struggle with images classified as deceiving by our methodology, models trained on our dataset maintain high performance on these challenging cases. Code and dataset are available at <https://github.com/mever-team/DiQuID>.*

1. Introduction

Image inpainting—the process of reconstructing missing or corrupted regions in images—has become increasingly accessible with the emergence of powerful generative AI tools, enabling even non-experts to create highly photo-

realistic edits [88]. In particular, text-guided image inpainting—the process of adding, removing, or altering specific regions in images using textual prompts—has seen remarkable advancement through models like Stable Diffusion [65], DALL-E [64], and Imagen [69]. These models allow users to add, remove, or alter content in images with high fidelity, using a textual description and a mask specifying the region to be edited.

While these developments offer new creative possibilities, they also present challenges regarding their potential misuse for malicious purposes, including the creation of deepfakes, and other deceptive media [78, 83]. Consequently, there is an increasing need for robust methods to detect and localize manipulated images to maintain trust and integrity in visual media [79, 93].

Image forgery detection techniques often rely on identifying inconsistencies in noise patterns, compression artifacts, or statistical irregularities in pixel distributions [4, 93]. However, modern generative models produce images that closely resemble natural images in terms of statistical properties, rendering many conventional detection approaches less effective [20]. Moreover, existing publicly available datasets for training and evaluating inpainting detection algorithms are limited in scale, diversity, or do not encompass the latest generative techniques [24, 55, 60]. For instance, datasets like MICC-F220 [1], DEFACTO [51], and CocoGlide [24] focus on outdated inpainting methods or comprise a limited number of low-resolution images.

Creating a high-quality dataset for inpainting detection involves two key challenges in automated generation. First, while state-of-the-art inpainting models are effective at image manipulation, they need detailed prompts for realistic results [50] - basic object labels often do not provide enough context for seamless integration. Second, evaluating image realism is difficult to automate, as standard quality metrics may not reflect how convincing the manipulations appear.

To address these challenges, we propose two key improvements to the dataset creation process. First, we use Large Language Models (LLMs) to create detailed, context-

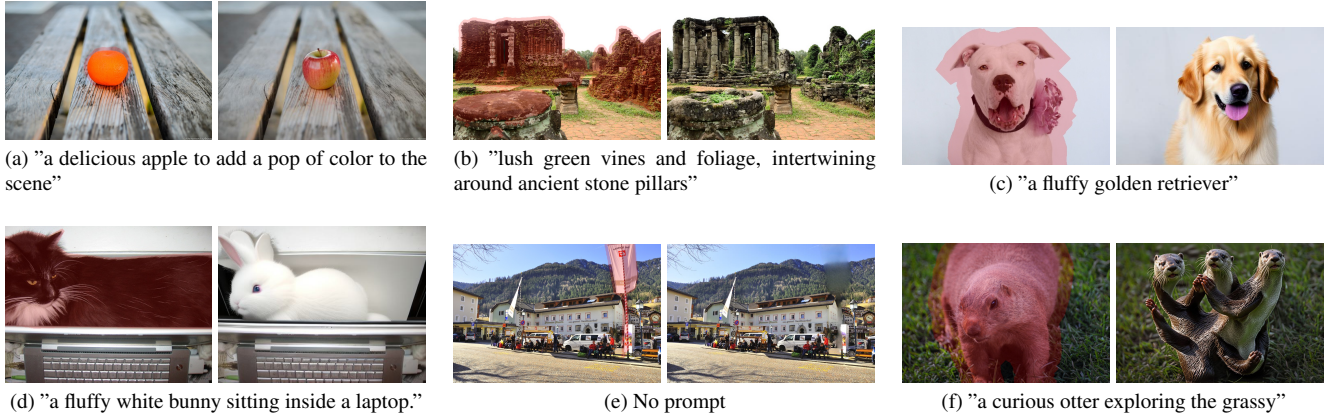


Figure 1. Original (with semi-transparent red inpainting mask) and inpainted images from three datasets, with prompts shown below each pair for text-guided models. The first row shows images classified as deceiving by UGDA 3.3, and the second row shows undeceiving images. Each column corresponds to a different dataset: COCO (first), RAISE (second), and OpenImages (third).

aware prompts that guide the inpainting process, producing results of higher aesthetic quality compared to simple object labels. Second, we develop a realism assessment method that uses vision-language models to compare inpainted images with their originals, helping identify convincing manipulations. Human studies validate this approach, showing it aligns with human perception of image realism.

Using this methodology, we create the *DiQuID* (**D**iversity and **Q**uality-aware **I**npainting **D**ataset) dataset for detecting AI-generated inpainting. The dataset contains 95,839 inpainted images generated from 78,684 original images from three datasets: MS-COCO [46], RAISE [18], and OpenImages [40]. We provide each inpainted image with its original version, inpainting mask, and text prompt. To ensure variety in manipulation types, we use multiple state-of-the-art diffusion-based inpainting models.

For thorough model evaluation, we create both in-domain and out-of-domain testing splits. The in-domain split uses the same LLM and source images as the training set, allowing assessment on familiar data. The out-of-domain split uses different source images and a different LLM, testing how well models handle new types of data.

Our main **contributions** are summarized as follows:

- We present the *DiQuID* dataset, the largest and most diverse dataset for AI-generated image inpainting detection to date, addressing the need for large-scale, high-quality data in this area.
- We propose a framework for generating contextually appropriate inpainted content by leveraging language models for prompt generation and multiple state-of-the-art inpainting pipelines mainly using diffusion models for image manipulation, supporting both spliced and fully re-generated manipulations
- We conduct extensive experiments comparing LLM-generated prompts to object class labels, demonstrating

superior aesthetic quality scores across multiple datasets, validating the effectiveness of our approach.

- We introduce an uncertainty-guided realism assessment methodology using vision-language models, validated through human studies showing strong correlation with perceived realism in manipulated images.
- We provide comprehensive benchmarking results across multiple state-of-the-art detection models, revealing significant performance gaps between in-domain (up to 0.69 IoU) and out-of-domain (0.23-0.66 IoU) scenarios, while demonstrating substantial improvements through retraining on our dataset.

2. Related Work

2.1. Image Inpainting

Early image inpainting methods used diffusion to simulate the restoration of an image region [7–10]. While later methods leveraged exemplar-based approaches for removing large objects from digital images [16, 25, 31, 35]. Recent image inpainting methods are deep learning-based, leveraging Convolutional Neural Networks (CNNs) [6], autoencoders [38], Generative Adversarial Networks (GANs) [22], Transformers [77], Diffusion Models [12], or some combination of these, and have significantly improved the quality and realism of inpainted regions. Early approaches demonstrated the potential of CNNs for inpainting tasks, sometimes incorporating frequency domain information through techniques like Fourier convolutions [73]. GAN-based methods have also been widely adopted, combining autoencoders and GANs to generate coherent images, with techniques such as Context Encoders [63] and dilated convolutions improving results [86]. Diffusion models have emerged as a powerful approach, using noise removal to reconstruct missing regions of images [49], with models

like GLIDE [57] and Stable Diffusion [66] incorporating additional guidance, such as text, for improved control. Other models, such as WavePaint [30], introduce wavelet transforms for efficient processing, while hybrid methods combining transformers and autoencoders have also shown promise in generating detailed reconstructions [19].

2.2. Inpainting Detection

The detection of inpainted regions in images has become increasingly important with the advances in inpainting methods. Early approaches focused on patch comparison and connectivity analysis to identify inconsistencies introduced by inpainting algorithms [11, 45, 84, 89]. These methods often draw inspiration from copy-move forgery detection frameworks, incorporating techniques such as Gabor magnitude analysis and color correlation [14, 32, 42, 52]. Machine learning-based approaches, such as SVM classifiers, rely on hand-crafted features [71]. Deep learning models, including CNN and ResNet [26] architectures, sometimes combined with Long Short-Term Memory (LSTM) Networks, showed better performance in distinguishing between modified and unmodified areas [39, 43, 48, 72, 94]. Recent developments introduced more complex architectures, such as hybrid transformer-CNN models and U-Net [67] variants, focusing on detecting noise inconsistencies and enhancing inpainting traces [67, 80, 92, 95]. Notable recent methods include SPAN [28], which uses a pyramidal self-attention structure, CFL-Net [58] using contrastive learning, and PSCC-Net [47] with its two-path model for feature extraction and mask enhancement. CatNet [41] uses Discrete Cosine Transform (DCT) coefficients and JPEG compression artifacts, while TruFor [24] combines RGB data with a noise-sensitive fingerprint (Noiseprint++ [15]) for robust alteration detection. MMFusion [76] extends TruFor by adding more filter convolutions, while others propose fusion architectures for combining semantic and low-level artifacts [34]. The FOCAL method [81] uses contrastive learning and unsupervised clustering to address the differentiation between forged and authentic regions. These approaches represent the current state-of-the-art in inpainting detection, offering both localization of altered areas and overall image tampering scores, improving the field’s ability to identify complex image manipulations [4, 16, 21].

2.3. Datasets for Image Inpainting Detection

The development and evaluation of inpainting detection models rely on diverse datasets that capture various inpainting techniques and scenarios. Early datasets such as MICC [1], CMFD [13], and CoFoMoD [75] focused primarily on copy-move forgeries, which can be considered a form of inpainting [3]. The Realistic Tampering Dataset [36, 37] introduced larger images and object removal forgeries, and was followed by the comprehensive MFC dataset [23] with

its widely used NIST16 subset [24, 41, 76, 81]. Specialized datasets emerged to address specific inpainting detection challenges, including DEFACTO [51], which covers multiple forgery types using MS COCO images [17, 46], IMD2020 [59] combining classic and learning-based inpainting methods [86], and DID/IID [80] incorporating various inpainting techniques. The rise of AI-generated content has led to datasets like CocoGlide [24] and TGIF [54], which utilize advanced models such as GLIDE, Stable Diffusion, and Adobe Firefly for inpainting.

3. Methodology

Creating a high-quality dataset for inpainting detection requires addressing three key challenges: ensuring semantic coherence in manipulations, maintaining diversity in inpainting approaches, and assessing the realism of generated images. To address these challenges, we propose a systematic methodology that carefully considers each aspect of the dataset creation process. Our approach combines language models for contextual understanding, multiple inpainting models for diverse manipulations, and vision-language models for quality assessment. This methodology consists of three main components: (1) Semantically Aligned Object Replacement (SAOR) that ensures contextually appropriate manipulations (Section 3.1), (2) Multi-Model Image Inpainting (MMII) that uses various state-of-the-art models for diverse modifications (Section 3.2), and (3) Uncertainty-Guided Deceptiveness Assessment (UGDA) that evaluates the realism of generated images (Section 3.3). Figure 2 shows the workflows of SAOR and MMII, while Figure 3 illustrates the workflow of UGDA.

3.1. Semantically Aligned Object Replacement (SAOR)

Generating realistic inpainting examples requires selecting appropriate objects for replacement and creating contextually relevant prompts that maintain semantic consistency with the image. To address this challenge, we propose Semantically Aligned Object Replacement (SAOR), a method that automates object selection and prompt generation.

Given an initial set of authentic images \mathcal{I} , SAOR processes each image through three stages. First, given $I_i \in \mathcal{I}$, object masks M_i and their respective labels O_i are obtained directly from labeled data if available; otherwise, a segmentation model $\Phi_{\text{seg}} : I_i \rightarrow (O_i, M_i)$ is used. Second, descriptive captions C_i are taken directly from labeled data if available; otherwise, they are generated by a captioning model $\Psi_{\text{cap}} : I_i \rightarrow C_i$. Finally, a language model $\Theta_{\text{llm}} : (C_i, O_i) \rightarrow (p_i, o_i)$ selects an object $o_j \in O_i$ (in text form) and generates a text prompt p_i to replace it. The language model, leveraging the caption to understand the image content, is instructed to produce complex, contextually

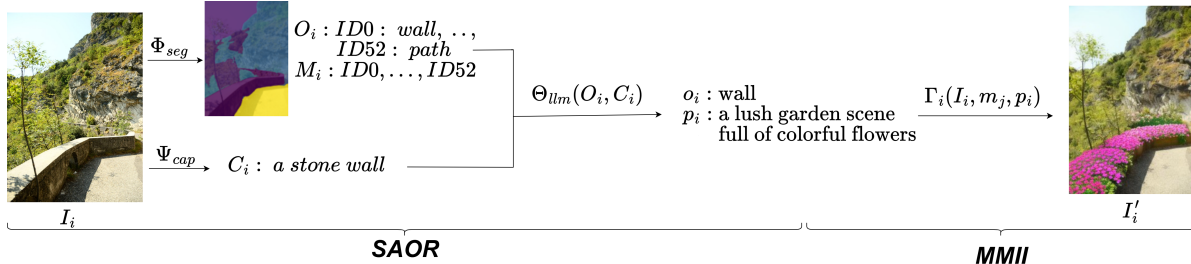


Figure 2. Overview of SAOR and MMII. The pipeline begins with an input image. The segmentation model Φ_{seg} performs instance segmentation, generating a list of objects. The captioning model Ψ_{cap} produces a caption for the image. The language model Θ_{llm} then uses the caption and object list to select an object and generate a prompt. Finally, the inpainting model Γ_j takes the image, the prompt, and a mask corresponding to the selected object to produce the inpainted result.

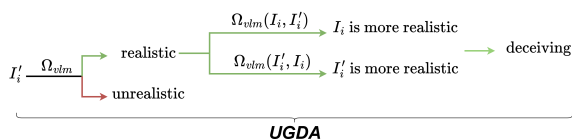


Figure 3. Overview of UGDA. Given an inpainted image I'_i , UGDA first evaluates its realism using Ω_{vlm} . If deemed realistic, UGDA performs a two-way comparison with the original image I_i to assess potential deceptiveness.

appropriate prompts, which enhance results [56, 68], maintaining semantic consistency with the surrounding content.

3.2. Multiple Model Image Inpainting (MMII)

The quality and diversity of inpainted images are crucial for creating a robust dataset for forgery detection. To achieve this, we employ multiple state-of-the-art inpainting models and various post-processing techniques, ensuring a wide range of realistic modifications.

Once the object $o_i \in O_i$ has been selected, with its corresponding mask $m_j \in M_i$, and the generated prompt p_i , we proceed to generate the inpainted image \hat{I}_i . We employ a set of state-of-the-art inpainting models $\Gamma = \Gamma_1, \dots, \Gamma_N$. Each inpainting model $\Gamma_j \in \Gamma$ receives an equal number of images for processing, with uniformly distributed settings such as diffusion models and post-processing techniques. Each model takes the original image I_i , the mask m_i , and the prompt p_i as inputs, producing the inpainted image as $\hat{I}_i = \Gamma_j(I_i, m_i, p_i)$. For diversity, a subset of images undergoes K additional rounds of inpainting using different models from Γ . The original, unprocessed images are retained for model training.

3.3. Uncertainty-Guided Deceptiveness Assessment (UGDA)

The quality of inpainted images must be assessed to create a meaningful dataset for forgery detection. To this end, we propose Uncertainty-guided Deceptiveness Assessment (UGDA), a process leveraging a Vision-Language Model

(VLM) that compares inpainted images with their originals. Let I_i denote the original image and \hat{I}_i the inpainted version of I_i . Using a vision-language model Ω_{vlm} , we perform the assessment in two stages.

Based on empirical observations, unrealistic manipulations were easily identifiable, while realistic ones required more thorough evaluation. \hat{I}_i undergoes the first UGDA stage where we ask the VLM if the image is realistic. For images passing the initial realism check, we introduce a comparative assessment leveraging two key insights: (1) when presented with both images, a VLM should more easily identify authentic content, so images where it fails to do so are likely more deceiving, and (2) a confident assessment should remain stable under input perturbations. A perturbation introducing variance to the assessment was input order. Thus, we perform two evaluations with reversed image order: $s_1 = \Omega_{vlm}(I_i, \hat{I}_i)$ and $s_2 = \Omega_{vlm}(\hat{I}_i, I_i)$, where $s_1, s_2 \in \{I_i, \hat{I}_i, \text{both}\}$. Any variation in responses indicates model uncertainty about \hat{I}_i 's realism.

The final classification follows these rules: \hat{I}_i is labeled as *deceiving* if $(s_1 = \hat{I}_i \vee s_2 = \hat{I}_i) \vee (s_1 = s_2 = \text{both})$. Otherwise, if both responses indicate I_i or one indicates I_i and the other *both*, \hat{I}_i is labeled as *undeceiving*. This approach enhances reliability in distinguishing between deceiving and easily identifiable synthetic images through uncertainty-aware, order-based evaluations. Figure 1 shows representative examples from UGDA across different sources. The first row demonstrates high-quality inpainting examples classified as *deceiving* by UGDA, where the manipulations are seamlessly integrated with the original content.

3.4. Implementation Details

Source of authentic data. To ensure diversity and robustness, we leverage datasets spanning multiple domains: general object detection, high-resolution photography, and large-scale segmentation. Specifically, we utilize three publicly available datasets for authentic image sources: (1) MS-

COCO [46], which provides images with captions and object masks across 80 categories (2) RAISE [18], a high-resolution dataset of 8,156 uncompressed RAW images designed for forgery detection evaluation (3) OpenImages [5], which offers extensive object segmentation data with over 2.7 million segmentations across 350 categories.

SAOR configuration. For SAOR, we use dataset-provided masks and captions for COCO and OpenImages, while for RAISE, we use OneFormer [29] as the segmentation model Φ_{seg} and BLIP-2 [44] as the captioning model Ψ_{cap} . For prompt generation, we use ChatGPT 3.5 [61] (for COCO/RAISE) and Claude Sonnet 3.5 [2] (for OpenImages) as the language model Θ_{llm} . The prompt engineering methodology is detailed in the supplementary material.

MMII configuration. For MMII, we utilize five inpainting pipelines (Γ): HD-Painter [53], BrushNet [33], PowerPaint [96], ControlNet [90], and Inpaint-Anything [87], along with its Remove-Anything variant for object removal. These pipelines collectively support eight inpainting models, primarily based on Stable Diffusion [66], except for Remove-Anything which employs LaMa architecture [73] based on CNNs and Fourier convolutions. Due to memory constraints, images were resized to a maximum dimension of 2048 pixels, except for the Inpaint Anything pipeline, which preserved original dimensions using cropping and resizing techniques. We perform $K = 2$ additional inpainting rounds on one-sixth of the images.

Preservation of unmasked area. We categorize inpainted images based on how models handle unmasked regions: if the unmasked region is preserved, we refer to them as Spliced (SP) images; if regenerated, as Fully Regenerated (FR) images. Inpaint-Anything preserves unmasked regions through copy-paste (SP), while ControlNet regenerates the full image (FR). BrushNet, PowerPaint, and HD-Painter can produce both SP and FR images depending on post-processing settings (e.g., blending or upscaling). Remove-Anything, based on LaMa architecture, inherently preserves unmasked regions, thus producing SP images. This diversity in processing approaches contributes to a more comprehensive dataset, as FR images are typically more challenging to detect than SP images [74].

UGDA configuration. For UGDA, we use GPT-4o [62] as the vision-language model Ω_{vlm} , chosen for its effectiveness in synthetic image detection [85]. The complete prompt engineering methodology is detailed in the supplementary material. Based on empirical observations that higher QAlign scores correlate with better inpainting quality and realism, we applied UGDA to approximately half of the test inpainted images, selecting those with the highest QAlign scores. The complete prompt engineering methodology is detailed in the supplementary material.

Dataset splits. As shown in Table 1, we structure our dataset to evaluate both in-domain performance and gen-

eralization to new data. For in-domain evaluation, we use COCO (60,000 randomly selected training images and nearly all 5,000 validation images for validation and testing) and RAISE (7,735 images processed with Φ_{seg} , yielding 25,674 image-mask-model combinations through 1-7 masks or prompts per image, with derived images kept in the same split, as each image was inpainted up to 4 times only in this dataset). To test generalization, we create an out-of-domain testing split using OpenImages—a dataset not used during training—comprising 6,000 randomly selected test images. This split uses a different language model Θ_{llm} (Claude) than COCO and RAISE (ChatGPT), providing a way to evaluate how well models perform on both new data and different prompting approaches. Throughout our experiments, we refer to the COCO and RAISE test splits as in-domain and the OpenImages test split as out-of-domain.

	Training	Validation	Testing
COCO [46]	59,708 (75%)	1,950 (31%)	2,922 (29%)
RAISE [18]	19,741 (25%)	4,262 (69%)	1,671 (16%)
OpenImages [5]	N/A	N/A	5,585 (55%)
Inpainted	79,449	6,212	10,178
Authentic	79,449	6,212	9,071

Table 1. Overview of dataset splits across COCO, RAISE, and OpenImages. The table shows the number of images in each split. The total number of images, including authentic and inpainted versions, is provided. Percentages represent the distribution of each dataset within the total split for inpainted images.

4. Experimental Evaluation

4.1. Experimental Setup

To establish a comprehensive benchmark for the presented *DiQuID* dataset, we evaluate the performance of several state-of-the-art image inpainting detection models.

Problem definition. Given an RGB image $x^{rgb} \in \mathbb{R}^{(H \times W \times 3)}$, the inpainting detection model aims to predict either a pixel-level inpainting localization mask $\hat{y}^{loc} \in (0, 1)^{(H \times W \times 1)}$ and/or an image-level inpainting detection probability $\hat{y}^{det} \in (0, 1)$. The former will be referred to as a localization problem, and the latter as a detection problem. All evaluations are conducted on the test sets.

Forensics models. For inpainting detection, we used four state-of-the-art models: PSCC [47], CAT-Net [41], TruFor [24], and MMFusion [76]. CAT-Net provides only a pixel-level localization mask, while the other models also output an image-level detection probability. For CAT-Net, image-level detection was evaluated by taking the maximum probability from the predicted localization mask.

Training protocol. We evaluated both pretrained models and versions retrained on the *DiQuID* dataset. This allowed us to compare the performance of the original models with their retrained counterparts.

Implementation Details. We retrained all models from scratch, following the training protocol outlined in their original papers. CAT-Net was trained on an NVIDIA A100 GPU, while PSCC, TruFor, and MMFusion were trained on an NVIDIA RTX 4090. Models were trained on the training set of *DiQuID* and the best checkpoints were selected based on validation set performance.

Evaluation metrics. We used distinct metrics to assess model performance at the image and pixel levels. For image-level evaluation (detection), we use accuracy to classify images as inpainted or not, with the positive class referring to inpainted regions. For pixel-level evaluation (localization), Intersection over Union (IoU) was used to measure the accuracy of localizing inpainted regions. In both cases, the threshold was arbitrarily set at 0.5.

4.2. Localization and Detection Results

We evaluate *DiQuID* by comparing the performance of four state-of-the-art inpainting detection models: PSCC, CAT-Net, TruFor, and MMFusion. We assess both pre-trained models and versions retrained on our dataset. Table 2 presents both the localization (IoU) and detection (accuracy) results for in-domain and out-of-domain testing sets and spliced (SP) and fully regenerated (FR) images.

Retraining on our dataset improves performance significantly. TruFor’s IoU increases from 0.12 to 0.65 for in-domain and 0.19 to 0.66 for out-of-domain testing. CAT-Net shows similar in-domain gains (0.39 to 0.69) but limited out-of-domain improvement (0.21 to 0.23). Domain generalization varies across models. While retrained CAT-Net achieves the highest in-domain IoU (0.69), it drops to 0.23 for out-of-domain. In contrast, retrained TruFor and PSCC maintain consistent performance across domains (0.65/0.66 and 0.58/0.58 respectively). The disconnect between IoU and accuracy metrics, particularly evident in the retrained CAT-Net’s results, suggests that high accuracy does not necessarily translate to precise localization of manipulated regions. SP detection is generally easier than FR, with retrained TruFor reaching 0.87 IoU on SP tasks. For FR images, most original models struggle (IoUs 0.06-0.20) but show clear improvements after retraining, with TruFor reaching 0.72 IoU. This suggests that detecting fully regenerated regions remains challenging, even for retrained models. TruFor’s strong performance likely stems from its pre-trained NoisePrint++ network, which enhances its ability to detect diverse manipulations. In contrast, CAT-Net and MMFusion may struggle with generalization due to their initial design for specific artifacts (e.g., JPEG compres-

sions) and added input complexities, respectively, which increase susceptibility to overfitting.

4.3. Model Compression Robustness Analysis

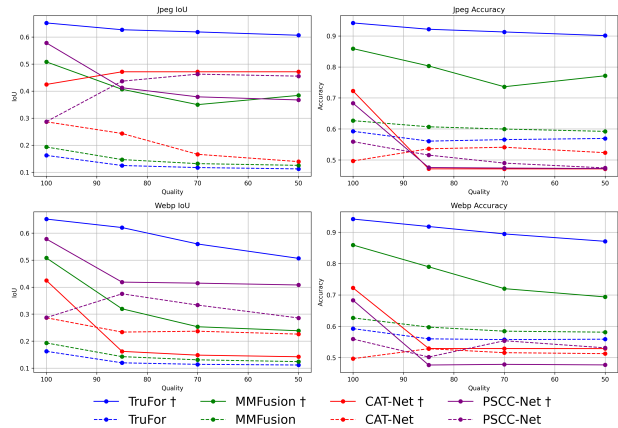


Figure 4. Robustness of model detection performance under compression. Top row shows model detection performance when subjected to JPEG compression at varying quality levels, while bottom row shows detection performance under WEBP compression.

We evaluate model robustness against JPEG and WEBP image compression at quality levels 0.85, 0.7, and 0.5. Figure 4 presents detection and localization results. Retrained TruFor shows the strongest resilience, maintaining stable performance across quality levels for both compression types. WEBP compression affects performance more than JPEG, particularly for localization tasks. All models show higher degradation in IoU scores compared to accuracy metrics, indicating that manipulation localization is more sensitive to compression artifacts than detection.

4.4. Ablation Studies

We conduct two ablations to validate our design choices. First, we evaluate SAOR’s use of language models by comparing LLM-generated prompts against simple object labels. Second, we assess UGDA’s effectiveness through a human study with 42 participants on 1,000 images, comparing human perception against model performance on images classified as *deceiving* or *undeceiving*.

Towards using language models. To justify the use of LLM-generated prompts in SAOR over simpler object label-based prompts, we processed a total of 900 original images (300 from each dataset), generating 4,500 images (900 from each of the five inpainting models) using LLM-generated prompts, and another 4,500 images using object class labels as prompts. We evaluated the aesthetics and quality of the generated images using metrics designed to align with human perception, including CLIP Similarity for Image Aesthetics [27] (referred to as CS, with “outstanding” and “atrocious” as positive and negative prompts),

Model	Mean IoU								Accuracy							
	ID		OOD		SP		FR		ID		OOD		SP		FR	
CAT-Net	0.39	0.21	0.41	0.06	0.60	0.42	0.85	0.40	0.60	0.42	0.85	0.40	0.60	0.42	0.85	0.40
CAT-Net†	0.69	+77%	0.23	+10%	0.47	+15%	0.36	+500%	0.99	+65%	0.53	+26%	1.00	+18%	1.00	+150%
PSCC	0.35	0.24	0.20	0.09	0.60	0.53	0.40	0.33	0.60	0.53	0.40	0.33	0.60	0.53	0.40	0.33
PSCC†	0.58	+66%	0.58	+142%	0.43	+115%	0.20	+122%	0.63	+5%	0.72	+36%	0.50	+25%	0.36	+9%
MMFusion	0.20	0.19	0.46	0.17	0.62	0.63	0.63	0.26	0.62	0.63	0.63	0.63	0.63	0.63	0.26	0.26
MMFusion†	0.64	+220%	0.41	+116%	0.73	+59%	0.50	+194%	0.93	+50%	0.81	+29%	0.86	+37%	0.82	+215%
TruFor	0.12	0.19	0.40	0.20	0.58	0.60	0.41	0.13	0.58	0.60	0.41	0.13	0.58	0.60	0.41	0.13
TruFor†	0.65	+442%	0.66	+247%	0.87	+117%	0.72	+260%	0.96	+66%	0.93	+55%	0.95	+132%	0.94	+623%

Table 2. Performance comparison of image forensics methods across domains. Evaluation metrics include Mean IoU and Accuracy for in-domain (ID), out-of-domain (OOD), SP, and FR images. Methods marked with † are retrained models, while unmarked ones are original. Bold values indicate column maxima, and percentages show retraining improvements.

Dataset	Quality				PSNR \uparrow		LPIPS $\times 10^3 \downarrow$		MSE $\times 10^3 \downarrow$		MAE $\times 10^3 \downarrow$		SSIM \uparrow	
	CS \uparrow	QA	QIt \uparrow	QA AE \uparrow	AS \uparrow	FR	SP	FR	SP	FR	SP	FR	SP	FR
Object Labels	0.33	4.16	2.66	5.56	27.37	104.89	37.82	0.56	5.92	0.01	37.29	0.85	0.85	1.00
LLM prompts	0.62	4.17	2.73	5.74	27.02	105.83	40.28	0.55	5.69	0.01	38.41	0.86	0.85	1.00
CocoGlide	-1.27	2.88	1.79	5.40	-	61.27	-	0.07	-	0.00	-	1.06	-	1.00
TGIF	-0.69	3.94	2.53	5.65	14.41	61.09	289.55	0.32	60.43	0.05	173.97	0.15	0.53	1.00
<i>DiQuID</i> (ours)	0.27	4.06	2.84	5.69	25.79	48.66	44.24	2.65	5.08	0.05	41.16	2.36	0.81	1.00

Table 3. Comparison of datasets based on quality, aesthetics, and fidelity metrics. The first two rows compare inpainting results when using prompts from LLMs versus directly using object labels under the same base settings. The last three rows compare our full dataset against existing datasets TGIF and Cocolgide. Metrics include quality assessments (QAlign Quality, QAlign Aesthetic, Aesthetic Score) and fidelity measures (PSNR, LPIPS, MSE, MAE, SSIM), with separate columns for FR and SP images.

Model	Accuracy				Mean IoU			
	All	Dec.	Int.	Und.	All	Dec.	Int.	Und.
Human	0.67	0.35	0.60	0.74	0.15	0.13	0.28	0.40
PSCC	0.52	0.30	0.38	0.29	0.29	0.15	0.14	0.14
CAT-Net	0.50	0.70	0.59	0.58	0.29	0.29	0.14	0.15
PSCC†	0.74	0.50	0.50	0.54	0.63	0.35	0.30	0.43
TruFor	0.60	0.35	0.25	0.22	0.17	0.35	0.25	0.27
MMFus	0.62	0.49	0.34	0.36	0.19	0.38	0.31	0.27
CAT-Net†	0.69	1.00	1.00	1.00	0.44	0.46	0.45	0.53
MMFus†	0.88	0.89	0.91	0.92	0.51	0.66	0.70	0.72
TruFor†	0.95	0.99	1.00	1.00	0.68	0.87	0.87	0.89

Table 4. Human vs. model performance comparison on inpainting detection. Results show accuracy and IoU for full test set (All) and images classified by UGDA as Deceiving (Dec.) or Undeceiving (Und.). † indicates models retrained on our dataset. Bold values indicate best performance per column.

QAlign for Quality Assessment (QA qtl) and Aesthetics Assessment (QA AE) [82], and Aesthetic Score [70]. In contrast, fidelity metrics such as Mean Squared Error (MSE), Mean Absolute Error (MAE), Peak Signal-to-Noise Ratio (PSNR), and Learned Perceptual Image Patch Similarity (LPIPS) [91] assess the preservation of the non-inpainted area. Fidelity metrics are most meaningful for FR images, whereas for SP images, where the compared areas are

nearly identical, they provide limited insight. The results, presented in the first two rows of Table 3, show that, on average, the images generated using LLM prompts yielded consistently higher aesthetic scores compared to those generated using object class labels, with benefits that solely only from prompt variations. Since all other settings remain unchanged (masks, inpainting models) technical metrics nearly identical between the two cases. This demonstrates the advantage of using LLMs for generating semantically rich and context-aware prompts.

UGDA human evaluation. To validate UGDA’s effectiveness and establish a human baseline, we conducted a comprehensive user study comparing human perception with model detection capabilities. We created a balanced evaluation set of 1,000 images: 250 classified as deceiving by UGDA, 250 as undeceiving, and 500 unaltered images as control. Images were randomly selected with constraints to avoid redundancy: no overlap between authentic images and originals of inpainted images, and no multiple inpainted versions from the same source. The study involved 42 participants evaluating batches of 20 images, with each image receiving 3-5 independent assessments. Participants included 26 males, 6 females, and 10 undisclosed. Ages ranged from 18 to 65+, with the largest group being 18-24

Model	Orig. Datasets	Original Images	Inp. Images	Inp. Models	Inp. Pipes	Double Inp.	Human Benchmark	Out-of-Domain Test Set	Type	Resolution
CocoGlide	1	512	512	1	✗	✗	✗	✗	AIGC	256 × 256
TGIF	1	3,124	74,976	3	✗	✗	✗	✗	AIGC	up to 1024p
DiQuID(ours)	3	77,900	95,839	8	5	✓	✓	✓	AIGC/OR	up to 2048p*

Table 5. Comparison of Inpainting Dataset Characteristics. Our dataset surpasses existing ones in scale (number of images), diversity (source datasets, models, pipelines). Resolution varies based on source dataset. The "Human Benchmark" column indicates whether a dataset includes a subset for human evaluation, while the "Out-of-Domain Test Set" column specifies whether the dataset contains images from distribution shifts for robustness assessment.

(19), followed by 25-34 (8) and 35-44 (6). Users were asked to detect inpainting and draw bounding boxes around suspected manipulated regions. For IoU computation, ground truth masks were converted to bounding boxes.

Table 4 presents the comparison between human evaluators and automated models. Human performance reached 0.69 accuracy and 0.15 IoU, significantly lower than re-trained models like TruFor (0.95 accuracy, 0.68 IoU) and MMFusion (0.88 accuracy, 0.51 IoU). Results are broken down into four categories: *All* represents performance on the complete test set, while *Deceiving*, *Undeceiving* and *Intermediate* correspond to UGDA’s classification of images based on their potential to fool human perception. The *Intermediate* category includes images that passed the initial realism check but not the second. Users particularly struggled with deceiving images (0.35 accuracy, 0.13 IoU) compared to undeceiving ones (0.74 accuracy, 0.40 IoU), validating UGDA’s effectiveness in identifying manipulations that are challenging for human perception. Also, the performance of humans on the intermediate category (0.60 accuracy, 0.28 IoU) confirms that the second stage is indeed efficient in discarding images that are not truly deceiving. In contrast, retrained models maintain high performance even on these challenging cases, with TruFor achieving 0.99 accuracy and 0.87 IoU on deceiving images. The performance gap between humans and models emphasizes the importance of automated detection methods, particularly for high-quality inpainting that can bypass human perception.

Quantitative comparison with state-of-the-art. To the best of our knowledge, *DiQuID* is the largest collection of AI-generated inpainted images. Table 5 presents a thorough comparison between our dataset and existing inpainting datasets in the field of AI-generated image detection. With 95,839 inpainted images derived from 77,900 originals, our dataset surpasses TGIF (74,976 from 3,124) and CocoGlide (512 from 512) in scale. Unlike existing datasets relying on a single source, ours integrates COCO, RAISE, and OpenImages, enhancing diversity. It also employs eight inpainting models across five pipelines, enabling complex manipulations, including double inpainting. Supporting resolutions up to 2048p, it exceeds TGIF’s 1024p and CocoGlide’s 256 × 256. Additionally, it uniquely includes a human benchmark subset and an out-of-domain test set,

reinforcing its value for evaluating inpainting detection under diverse and challenging conditions. As shown in Table 3, our dataset demonstrates superior performance in aesthetic, quality, and fidelity metrics compared to existing datasets. This indicates that our dataset achieves higher perceptual alignment with human judgment (CS, QA Alt, QA AE, AS) and better preservation of the non-inpainted areas (PSNR, LPIPS, MSE, MAE, SSIM) in FR cases, where it is most relevant. By combining AI-generated image content (AIGC) and object removal (OR) techniques, our dataset offers a comprehensive benchmark that supports inpainting detection across a wider range of manipulation scenarios. This approach positions our dataset as a superior resource for advancing inpainting detection models and sets a new standard for benchmarking in the field.

5. Conclusions and Future work

We presented *DiQuID*, a large-scale dataset for evaluating inpainting detection methods, built using a novel pipeline with three key components: SOAR for semantic-aware object selection, MMII for diverse inpainting manipulations, and UGDA for deceptiveness assessment. Built to be model-agnostic, our approach can integrate future improvements in segmentation, captioning, and language models. Unlike previous datasets, our approach leverages multiple state-of-the-art inpainting pipeline and uses language models to generate contextually rich prompts, enhancing the aesthetic and technical quality of manipulated images. Our benchmarking reveals both strengths and limitations of current detection methods, particularly for FR images and compressed images. Looking forward, our framework can benefit from advances in foundation models to improve prompt generation, realism assessment, and object selection. Future work should focus on developing detection architectures that are robust to compression while maintaining accurate localization of manipulated regions. We hope *DiQuID* will drive progress in developing more robust forgery detection methods as AI-generated content proliferates.

Acknowledgments: This work was supported by the Horizon Europe vera.ai project (grant no.101070093) and by the High Performance Computing infrastructure of the Aristotle University of Thessaloniki.

References

- [1] Irene Amerini, Lamberto Ballan, Roberto Caldelli, Alberto Del Bimbo, and Giuseppe Serra. A sift-based forensic method for copy-move attack detection and transformation recovery. *IEEE Transactions on Information Forensics and Security*, 6(3):1099–1110, 2011. 1, 3
- [2] Anthropic. Claude 3.5 sonnet, 2024. Large Language Model. 5
- [3] Adrian-Alin Barglazan, Remus Brad, and Constantin Constantinescu. Image inpainting forgery detection: a review. *Journal of Imaging*, 10(2):42, 2024. 3
- [4] Belhassen Bayar and Matthew C. Stamm. A deep learning approach to universal image manipulation detection using a new convolutional layer. In *Proceedings of the 4th ACM Workshop on Information Hiding and Multimedia Security*. ACM, 2016. 1, 3
- [5] Rodrigo Benenson and Vittorio Ferrari. From coloring-in to pointillism: revisiting semantic segmentation supervision. In *ArXiv*, 2022. 5
- [6] Y. Bengio and Yann Lecun. Convolutional networks for images, speech, and time-series, 1997. 2
- [7] M. Bertalmio. Contrast invariant inpainting with a 3rd order, optimal pde. In *IEEE International Conference on Image Processing 2005*, pages II–778, 2005. 2
- [8] Marcelo Bertalmio, Guillermo Sapiro, Vincent Caselles, and Coloma Ballester. Image inpainting. In *Proceedings of the 27th Annual Conference on Computer Graphics and Interactive Techniques*, page 417–424, USA, 2000. ACM Press/Addison-Wesley Publishing Co.
- [9] M. Bertalmio, A.L. Bertozzi, and G. Sapiro. Navier-stokes, fluid dynamics, and image and video inpainting. In *Proceedings of the 2001 IEEE Computer Society Conference on Computer Vision and Pattern Recognition. CVPR 2001*, pages I–I, 2001.
- [10] Tony F. Chan and Jianhong Shen. Nontexture inpainting by curvature-driven diffusions. *Journal of Visual Communication and Image Representation*, 12(4):436–449, 2001. 2
- [11] I-Cheng Chang, J. Cloud Yu, and Chih-Chuan Chang. A forgery detection algorithm for exemplar-based inpainting images using multi-region relation. *Image and Vision Computing*, 31(1):57–71, 2013. 3
- [12] Ziyi Chang, George Alex Koulieris, and Hubert P. H. Shum. On the design fundamentals of diffusion models: A survey, 2023. 2
- [13] Vincent Christlein, Christian Riess, Johannes Jordan, Corinna Riess, and Elli Angelopoulou. An evaluation of popular copy-move forgery detection approaches. *IEEE Transactions on Information Forensics and Security*, 7(6):1841–1854, 2012. 3
- [14] Vincent Christlein, Christian Riess, Johannes Jordan, Corinna Riess, and Elli Angelopoulou. An evaluation of popular copy-move forgery detection approaches. *IEEE Transactions on Information Forensics and Security*, 7(6):1841–1854, 2012. 3
- [15] Davide Cozzolino and Luisa Verdoliva. Noiseprint: A cnn-based camera model fingerprint. *IEEE Transactions on Information Forensics and Security*, 15:144–159, 2020. 3
- [16] A. Criminisi, P. Perez, and K. Toyama. Region filling and object removal by exemplar-based image inpainting. *IEEE Transactions on Image Processing*, 13(9):1200–1212, 2004. 2, 3
- [17] M. Daisy, P. Buysens, D. Tschumperlé, and O. Lézoray. A smarter exemplar-based inpainting algorithm using local and global heuristics for more geometric coherence. In *2014 IEEE International Conference on Image Processing (ICIP)*, pages 4622–4626, 2014. 3
- [18] Duc-Tien Dang-Nguyen, Cecilia Pasquini, Valentina Conotter, and Giulia Boato. Raise: a raw images dataset for digital image forensics. In *Proceedings of the 6th ACM Multimedia Systems Conference*, page 219–224, New York, NY, USA, 2015. Association for Computing Machinery. 2, 5
- [19] Patrick Esser, Robin Rombach, and Björn Ommer. Taming transformers for high-resolution image synthesis. In *2021 IEEE/CVF Conference on Computer Vision and Pattern Recognition (CVPR)*, pages 12868–12878, 2021. 3
- [20] Joel Frank, Thorsten Eisenhofer, Lea Schönherr, Asja Fischer, Dorothea Kolossa, and Thorsten Holz. Leveraging frequency analysis for deep fake image recognition, 2020. 1
- [21] Jessica Fridrich and Jan Kodovsky. Rich models for steganalysis of digital images. *IEEE Transactions on Information Forensics and Security*, 7(3):868–882, 2012. 3
- [22] Ian J. Goodfellow, Jean Pouget-Abadie, Mehdi Mirza, Bing Xu, David Warde-Farley, Sherjil Ozair, Aaron Courville, and Yoshua Bengio. Generative adversarial networks, 2014. 2
- [23] Haiying Guan, Mark Kozak, Eric Robertson, Yooyoung Lee, Amy N. Yates, Andrew Delgado, Daniel Zhou, Timothee Kheyrkhan, Jeff Smith, and Jonathan Fiscus. Mfc datasets: Large-scale benchmark datasets for media forensic challenge evaluation. In *2019 IEEE Winter Applications of Computer Vision Workshops (WACVW)*, pages 63–72, 2019. 3
- [24] Fabrizio Guillaro, Davide Cozzolino, Avneesh Sud, Nicholas Dufour, and Luisa Verdoliva. Trufor: Leveraging all-round clues for trustworthy image forgery detection and localization, 2023. 1, 3, 5
- [25] Qiang Guo, Shanshan Gao, Xiaofeng Zhang, Yilong Yin, and Caiming Zhang. Patch-based image inpainting via two-stage low rank approximation. *IEEE Transactions on Visualization and Computer Graphics*, 24(6):2023–2036, 2018. 2
- [26] Kaiming He, Xiangyu Zhang, Shaoqing Ren, and Jian Sun. Deep residual learning for image recognition, 2015. 3
- [27] Simon Hentschel, Konstantin Kobs, and Andreas Hotho. Clip knows image aesthetics. *Frontiers in Artificial Intelligence*, 5, 2022. 6
- [28] Xuefeng Hu, Zhihan Zhang, Zhenye Jiang, Syomantak Chaudhuri, Zhenheng Yang, and Ram Nevatia. Span: Spatial pyramid attention network for image manipulation localization. In *Computer Vision – ECCV 2020*, pages 312–328, Cham, 2020. Springer International Publishing. 3
- [29] Jitesh Jain, Jiachen Li, MangTik Chiu, Ali Hassani, Nikita Orlov, and Humphrey Shi. Oneformer: One transformer to rule universal image segmentation, 2022. 5
- [30] Pranav Jeevan, Dharshan Sampath Kumar, and Amit Sethi. Wavepaint: Resource-efficient token-mixer for self-supervised inpainting, 2023. 3

- [31] Kyong Hwan Jin and Jong Chul Ye. Annihilating filter-based low-rank hankel matrix approach for image inpainting. *IEEE Transactions on Image Processing*, 24(11):3498–3511, 2015. 2
- [32] Xiao Jin, Yuting Su, Liang Zou, Yongwei Wang, Peiguang Jing, and Z. Jane Wang. Sparsity-based image inpainting detection via canonical correlation analysis with low-rank constraints. *IEEE Access*, 6:49967–49978, 2018. 3
- [33] Xuan Ju, Xian Liu, Xintao Wang, Yuxuan Bian, Ying Shan, and Qiang Xu. Brushnet: A plug-and-play image inpainting model with decomposed dual-branch diffusion, 2024. 5
- [34] Dimitrios Karageorgiou, Giorgos Kordopatis-Zilos, and Symeon Papadopoulos. Fusion transformer with object mask guidance for image forgery analysis. In *Proceedings of the IEEE/CVF Conference on Computer Vision and Pattern Recognition*, pages 4345–4355, 2024. 3
- [35] Norihiko Kawai, Tomokazu Sato, and Naokazu Yokoya. Diminished reality based on image inpainting considering background geometry. *IEEE Transactions on Visualization and Computer Graphics*, 22(3):1236–1247, 2016. 2
- [36] P. Korus and J. Huang. Evaluation of random field models in multi-modal unsupervised tampering localization. In *Proc. of IEEE Int. Workshop on Inf. Forensics and Security*, 2016. 3
- [37] P. Korus and J. Huang. Multi-scale analysis strategies in prnu-based tampering localization. *IEEE Trans. on Information Forensics & Security*, 2017. 3
- [38] Mark A. Kramer. Nonlinear principal component analysis using autoassociative neural networks. *AICHE Journal*, 37(2):233–243, 1991. 2
- [39] Nitish Kumar and Toshnall Meenpal. Semantic segmentation-based image inpainting detection. In *Innovations in Electrical and Electronic Engineering*, pages 665–677, Singapore, 2021. Springer Singapore. 3
- [40] Alina Kuznetsova et al. The open images dataset v4: Unified image classification, object detection, and visual relationship detection at scale. *International Journal of Computer Vision*, 128(7):1956–1981, 2020. 2
- [41] Myung-Joon Kwon, Seung-Hun Nam, In-Jae Yu, Heung-Kyu Lee, and Changick Kim. Learning jpeg compression artifacts for image manipulation detection and localization. *International Journal of Computer Vision*, 130(8):1875–1895, 2022. 3, 5
- [42] Jen-Chun Lee. Copy-move image forgery detection based on gabor magnitude. *Journal of Visual Communication and Image Representation*, 31:320–334, 2015. 3
- [43] Haodong Li and Jiwu Huang. Localization of deep inpainting using high-pass fully convolutional network. In *2019 IEEE/CVF International Conference on Computer Vision (ICCV)*, pages 8300–8309, 2019. 3
- [44] Junnan Li, Dongxu Li, Silvio Savarese, and Steven Hoi. Blip-2: Bootstrapping language-image pre-training with frozen image encoders and large language models, 2023. 5
- [45] Zaoshan Liang, Gaobo Yang, Xiangling Ding, and Leida Li. An efficient forgery detection algorithm for object removal by exemplar-based image inpainting. *Journal of Visual Communication and Image Representation*, 30:75–85, 2015. 3
- [46] Tsung-Yi Lin, Michael Maire, Serge Belongie, James Hays, Pietro Perona, Deva Ramanan, Piotr Dollár, and C. Lawrence Zitnick. Microsoft coco: Common objects in context. In *Computer Vision – ECCV 2014*, pages 740–755, Cham, 2014. Springer International Publishing. 2, 3, 5
- [47] Xiaohong Liu, Yaojie Liu, Jun Chen, and Xiaoming Liu. Psc-net: Progressive spatio-channel correlation network for image manipulation detection and localization. *IEEE Transactions on Circuits and Systems for Video Technology*, 32(11):7505–7517, 2022. 3, 5
- [48] Ming Lu and Shaozhang Niu. A detection approach using lstm-cnn for object removal caused by exemplar-based image inpainting. *Electronics*, 9(5), 2020. 3
- [49] Andreas Lugmayr, Martin Danelljan, Andres Romero, Fisher Yu, Radu Timofte, and Luc Van Gool. Repaint: Inpainting using denoising diffusion probabilistic models. In *2022 IEEE/CVF Conference on Computer Vision and Pattern Recognition (CVPR)*, pages 11451–11461, 2022. 2
- [50] Shweta Mahajan, Tanzila Rahman, Kwang Moo Yi, and Leonid Sigal. Prompting hard or hardly prompting: Prompt inversion for text-to-image diffusion models, 2023. 1
- [51] Gaël MAHFOUDI, Badr TAJINI, Florent RETRAINT, Frédéric MORAIN-NICOLIER, Jean Luc DUGELAY, and Marc PIC. Defacto: Image and face manipulation dataset. In *2019 27th European Signal Processing Conference (EUSIPCO)*, pages 1–5, 2019. 1, 3
- [52] Gaël MAHFOUDI, Frédéric MORAIN-NICOLIER, Florent RETRAINT, and Marc PIC. Object-removal forgery detection through reflectance analysis. In *2020 IEEE International Symposium on Signal Processing and Information Technology (ISSPIT)*, pages 1–6, 2020. 3
- [53] Ara Manukyan. Hd-painter: High-resolution prompt-faithful text-guided image inpainting, 2024. 5
- [54] Hannes Mareen, Dimitrios Karageorgiou, Glenn Van Walendael, Peter Lambert, and Symeon Papadopoulos. Tgif: Text-guided inpainting forgery dataset, 2024. 3
- [55] Hugo Mareen et al. Tgif: A text-guided image forgery dataset for deepfake detection. *arXiv preprint arXiv:2401.56789*, 2024. 1
- [56] Oscar Mañas, Pietro Astolfi, Melissa Hall, Candace Ross, Jack Urbanek, Adina Williams, Aishwarya Agrawal, Adriana Romero-Soriano, and Michal Drozdal. Improving text-to-image consistency via automatic prompt optimization, 2024. 4
- [57] Alex Nichol, Prafulla Dhariwal, Aditya Ramesh, Pranav Shyam, Pamela Mishkin, Bob McGrew, Ilya Sutskever, and Mark Chen. Glide: Towards photorealistic image generation and editing with text-guided diffusion models, 2022. 3
- [58] Fahim Faisal Niloy, Kishor Kumar Bhaumik, and Simon S. Woo. Cfl-net: Image forgery localization using contrastive learning, 2022. 3
- [59] Adam Novozamsky, Babak Mahdian, and Stanislav Saic. Imd2020: A large-scale annotated dataset tailored for detecting manipulated images. In *2020 IEEE Winter Applications of Computer Vision Workshops (WACVW)*, pages 71–80, 2020. 3

- [60] Jan Novozámský, Gertjan Meuleman, et al. Imd2020: A large-scale annotated dataset tailored for image manipulation detection. In *Proceedings of the 25th International Conference on Pattern Recognition*, pages 2749–2756, 2021. 1
- [61] OpenAI. Chatgpt-3.5, 2023. 5
- [62] OpenAI. Chatgpt-4, 2023. 5
- [63] Deepak Pathak, Philipp Krähenbühl, Jeff Donahue, Trevor Darrell, and Alexei A. Efros. Context encoders: Feature learning by inpainting. In *2016 IEEE Conference on Computer Vision and Pattern Recognition (CVPR)*, pages 2536–2544, 2016. 2
- [64] Aditya Ramesh, Mikhail Pavlov, Gabriel Goh, Scott Gray, Chelsea Voss, Alec Radford, Mark Chen, and Ilya Sutskever. Zero-shot text-to-image generation. In *Proceedings of the International Conference on Machine Learning*, pages 8821–8831, 2021. 1
- [65] Robin Rombach, Andreas Blattmann, Dominik Lorenz, Patrick Esser, and Björn Ommer. High-resolution image synthesis with latent diffusion models. In *Proceedings of the IEEE/CVF Conference on Computer Vision and Pattern Recognition*, pages 10684–10695, 2022. 1
- [66] Robin Rombach, Andreas Blattmann, Dominik Lorenz, Patrick Esser, and Björn Ommer. High-resolution image synthesis with latent diffusion models, 2022. 3, 5
- [67] Olaf Ronneberger, Philipp Fischer, and Thomas Brox. U-net: Convolutional networks for biomedical image segmentation, 2015. 3
- [68] Shachar Rosenman, Vasudev Lal, and Phillip Howard. Neuprompts: An adaptive framework to optimize prompts for text-to-image generation, 2024. 4
- [69] Chitwan Saharia, William Chan, Saurabh Saxena, Lala Li, Jay Whang, Emily Denton, Seyed Kamyar Seyed Ghasemipour, Burcu Karagol Ayan, S Sara Mahdavi, and Raphael Gontijo Lopes. Photorealistic text-to-image diffusion models with deep language understanding. *arXiv preprint arXiv:2205.11487*, 2022. 1
- [70] Christoph Schuhmann, Romain Beaumont, Richard Vencu, Cade Gordon, Ross Wightman, Mehdi Cherti, Theo Coombes, Aarush Katta, Clayton Mullis, Mitchell Wortsman, Patrick Schramowski, Srivatsa Kundurthy, Katherine Crowson, Ludwig Schmidt, Robert Kaczmarczyk, and Jenia Jitsev. Laion-5b: An open large-scale dataset for training next generation image-text models, 2022. 7
- [71] Linchuan Shen, Gaobo Yang, Leida Li, and Xingming Sun. Robust detection for object removal with post-processing by exemplar-based image inpainting. In *2017 13th International Conference on Natural Computation, Fuzzy Systems and Knowledge Discovery (ICNC-FSKD)*, pages 2730–2736, 2017. 3
- [72] Karen Simonyan and Andrew Zisserman. Very deep convolutional networks for large-scale image recognition, 2015. 3
- [73] Roman Suvorov, Elizaveta Logacheva, Anton Mashikhin, Anastasia Remizova, Arsenii Ashukha, Aleksei Silvestrov, Naejin Kong, Harshith Goka, Kiwoong Park, and Victor Lempitsky. Resolution-robust large mask inpainting with fourier convolutions, 2021. 2, 5
- [74] Matías Tailanian, Marina Gardella, Álvaro Pardo, and Pablo Musé. Diffusion models meet image counter-forensics, 2024. 5
- [75] Dijana Tralic, Ivan Zupancic, Sonja Grgic, and Mislav Grgic. Comofod — new database for copy-move forgery detection. In *Proceedings ELMAR-2013*, pages 49–54, 2013. 3
- [76] Konstantinos Triaridis and Vasileios Mezaris. Exploring multi-modal fusion for image manipulation detection and localization, 2023. 3, 5
- [77] Ashish Vaswani, Noam Shazeer, Niki Parmar, Jakob Uszkoreit, Llion Jones, Aidan N. Gomez, Lukasz Kaiser, and Illia Polosukhin. Attention is all you need, 2023. 2
- [78] Luisa Verdoliva. Media forensics and deepfakes: An overview. *IEEE Journal of Selected Topics in Signal Processing*, 14(5):910–932, 2020. 1
- [79] Yuan Wang et al. A cnn-based framework for passive image copy-move forgery detection. *Pattern Recognition Letters*, 70:35–42, 2016. 1
- [80] Haiwei Wu and Jiantao Zhou. Iid-net: Image inpainting detection network via neural architecture search and attention. *IEEE Transactions on Circuits and Systems for Video Technology*, 32(3):1172–1185, 2022. 3
- [81] Haiwei Wu, Yiming Chen, and Jiantao Zhou. Rethinking image forgery detection via contrastive learning and unsupervised clustering, 2023. 3
- [82] Haoning Wu, Zicheng Zhang, Weixia Zhang, Chaofeng Chen, Liang Liao, Chunyi Li, Yixuan Gao, Annan Wang, Erli Zhang, Wenxiu Sun, Qiong Yan, Xiongkuo Min, Guangtao Zhai, and Weisi Lin. Q-align: Teaching lms for visual scoring via discrete text-defined levels, 2023. 7
- [83] Pin-Yu Wu, C-C Jay Kuo, et al. Defakehop: A light-weight high-performance deepfake detector. *IEEE Transactions on Multimedia*, 24:343–353, 2022. 1
- [84] Qiong Wu, Shao-Jie Sun, Wei Zhu, Guo-Hui Li, and Dan Tu. Detection of digital doctoring in exemplar-based inpainted images. In *2008 International Conference on Machine Learning and Cybernetics*, pages 1222–1226, 2008. 3
- [85] Junyan Ye, Baichuan Zhou, Zilong Huang, Junan Zhang, Tianyi Bai, Hengrui Kang, Jun He, Honglin Lin, Zihao Wang, Tong Wu, Zhizheng Wu, Yiping Chen, Dahua Lin, Conghui He, and Weijia Li. Loki: A comprehensive synthetic data detection benchmark using large multimodal models, 2024. 5
- [86] Jiahui Yu, Zhe Lin, Jimei Yang, Xiaohui Shen, Xin Lu, and Thomas S. Huang. Generative image inpainting with contextual attention, 2018. 2, 3
- [87] Tao Yu, Runseng Feng, Ruoyu Feng, Jinming Liu, Xin Jin, Wenjun Zeng, and Zhibo Chen. Inpaint anything: Segment anything meets image inpainting, 2023. 5
- [88] Chenshuang Zhang, Chaoning Zhang, Mengchun Zhang, In So Kweon, and Junmo Kim. Text-to-image diffusion models in generative ai: A survey, 2024. 1
- [89] Dengyong Zhang, Zaoshan Liang, Gaobo Yang, Qingguo Li, Leida Li, and Xingming Sun. A robust forgery detection algorithm for object removal by exemplar-based image inpainting. *Multimedia Tools and Applications*, 77(10):11823–11842, 2018. 3

- [90] Lvmin Zhang, Anyi Rao, and Maneesh Agrawala. Adding conditional control to text-to-image diffusion models, 2023. 5
- [91] Richard Zhang, Phillip Isola, Alexei A. Efros, Eli Shechtman, and Oliver Wang. The unreasonable effectiveness of deep features as a perceptual metric, 2018. 7
- [92] Yushu Zhang, Zhibin Fu, Shuren Qi, Mingfu Xue, Zhongyun Hua, and Yong Xiang. Localization of inpainting forgery with feature enhancement network. *IEEE Transactions on Big Data*, 9(3):936–948, 2023. 3
- [93] Peng Zhou, Weidi Han, Vlad I Morariu, and Larry S Davis. Learning rich features for image manipulation detection. In *Proceedings of the IEEE Conference on Computer Vision and Pattern Recognition*, pages 1053–1061, 2018. 1
- [94] Xinshan Zhu, Yongjun Qian, Xianfeng Zhao, Biao Sun, and Ya Sun. A deep learning approach to patch-based image inpainting forensics. *Signal Processing: Image Communication*, 67:90–99, 2018. 3
- [95] Xinshan Zhu, Junyan Lu, Honghao Ren, Hongquan Wang, and Biao Sun. A transformer–cnn for deep image inpainting forensics. *The Visual Computer*, 39(10):4721–4735, 2023. 3
- [96] Junhao Zhuang, Yanhong Zeng, Wenran Liu, Chun Yuan, and Kai Chen. A task is worth one word: Learning with task prompts for high-quality versatile image inpainting, 2024. 5